Imaging of Oriented Molecules†

M. H. M. Janssen,* J. W. G. Mastenbroek, and S. Stolte

Department of Chemistry, Vrije Universiteit, De Boelelaan 1083, 1081 HV Amsterdam, The Netherlands

Received: April 3, 1997; In Final Form: June 10, 1997⊗

Hexapole state selection and orientation of parent molecules is combined with two-dimensional ion imaging of photofragments to study the direct photolysis of deuterated methyl iodide molecules (CD_3I) at 266 nm. The combination of these two techniques allows us to create an essentially single quantum state-selected beam of oriented molecules, which are subsequently photodissociated, and to measure the final state-, velocity-, and angle-resolved recoil distribution of the photofragments. Extensive measurements have been done on the variation of the recoil distribution with the orientation field strength applied. These measurements allow a quantitative comparison of the orientation distribution of state-selected methyl iodide molecules with theoretical Stark effect calculations. For the prompt dissociation of CD_3I at 266 nm the angular recoil distribution of the $I(^2P_{1/2})$ photofragment reflects predominantly the initial spatial orientation of the state-selected parent. A comparison is presented between the fragment recoil distributions when different initial oriented parent states are selected.

1. Introduction

The study of photodissociation dynamics has been of great importance in elucidating the role of intramolecular (anisotropic) forces and in determining the shape of the potential surfaces which are involved in the photodynamics. One of the experimental observables in photodissociation processes is the spatial angular recoil distribution of the photofragments. The angular recoil distribution of the photofragments provides information about the nature of the photoabsorption process and the subsequent dynamics on the excited state surface. In the case of randomly oriented parent molecules the departure of the recoil distribution from spherical symmetry is described by the so-called β-parameter.[1] As has been discussed before,[2−4] the anisotropy parameter β is the product of two Legendre moments: one moment reflects the symmetry of the absorption process; the other moment gives information about the recoil distribution in the molecular frame. However, in the case of an oriented parent molecule one can, in principle, seperate these two contributions. Choi and Bernstein[5] and Zare[6] showed mathematically how the angular recoil distribution for a prompt axial recoil reflects the prepared orientational distribution of the parent molecule. Taatjes *et al.*[7] generalized this treatment for arbitrary recoil dynamics and showed how using oriented parent molecules one can, in principle, obtain more details of the molecular frame recoil distribution and go beyond the mere extraction of the prepared wave function of the oriented parent. Recently, Seideman[8] discussed, using a quantum mechanical time-independent method, the information content of magnetic-state-selected photodissociation and showed[9] how the exact quantum mechanical expressions for the angular distribution in the limit of a rapid dissociation reduce to the more phenomenologically derived expressions of refs 5 and 6.

Since the start of experiments employing oriented molecules, it was evident that, in order to interpret the results of *e.g.* steric effects in bimolecular reactive scattering correctly, a good knowledge about the orientational distribution of the oriented reagent was a prerequisite.[10] The hexapole method was used almost exclusively to obtain oriented molecules untill the advance of the brute-force method[11,12] several years ago. In the middle 1980s[13,14] it was demonstrated that the hexapole method was able to produce beams of almost pure single-state-selected symmetric top molecules. Using these single-state-selected beams, it now became possible to test (indirectly) the obtained orientational distribution more quantitatively. By measuring *e.g.* the orientation field dependence of the steric effect of the chemiluminescent reactive product yield[15,16] and comparing this with Stark effect calculations, it was inferred how well the reactant was oriented experimentally.

Of course, one would like to measure these distributions more directly. Bernstein and co-workers[17,18] used the photodissociation of oriented methyl iodide with time-of-flight (TOF) arrival time detection of $I(^2P_{1/2})$ photofragments to obtain the forward−backward degree of orientation of the parent molecules. In the analysis of this data it was found that a rigorous quantitative comparison of the experimental data with calculated distributions suffered from background problems, inherent to the detection method used. The experiments on photodissociation of hexapole state-selected and oriented methyl iodide with TOF detection have been extended recently by the group of Baugh to extract transition dipole matrix elements from the TOF data.[19] Using the same techniques, they also studied the photofragmentation of ND_3.[20] Kasai and co-workers[21] reported a beam-intensity-depletion method to determine the direction of the transition dipole moment in the photolysis of oriented CH_3I. Recently, Böwering and co-workers[22] reported electron diffraction experiments on state-selected and oriented methyl halides. Because of a relatively warm molecular beam without single state selection and the presence of an electron beam, they cannot apply large enough voltages to fully orient their sample, which makes quantitative comparison of the results somewhat complex. Employing the so-called brute-force method, Miller and co-workers studied the photofragment angular distributions of dc oriented "pendular" states of van der Waals clusters like N_2−HF.[23]

In this paper we present results employing a more advanced photofragment technique, the so-called ion imaging technique,[24,25] to study the orientation distribution of oriented methyl

‡ E-mail address: mhmj@chem.vu.nl.

† Dedicated to the late Prof. R. B. Bernstein who initiated the attempts of measuring the orientation of molecules via a prompt photodissociation along the molecular axis.

⊗ Abstract published in *Advance ACS Abstracts,* September 1, 1997.

S1089-5639(97)01159-6 CCC: $14.00

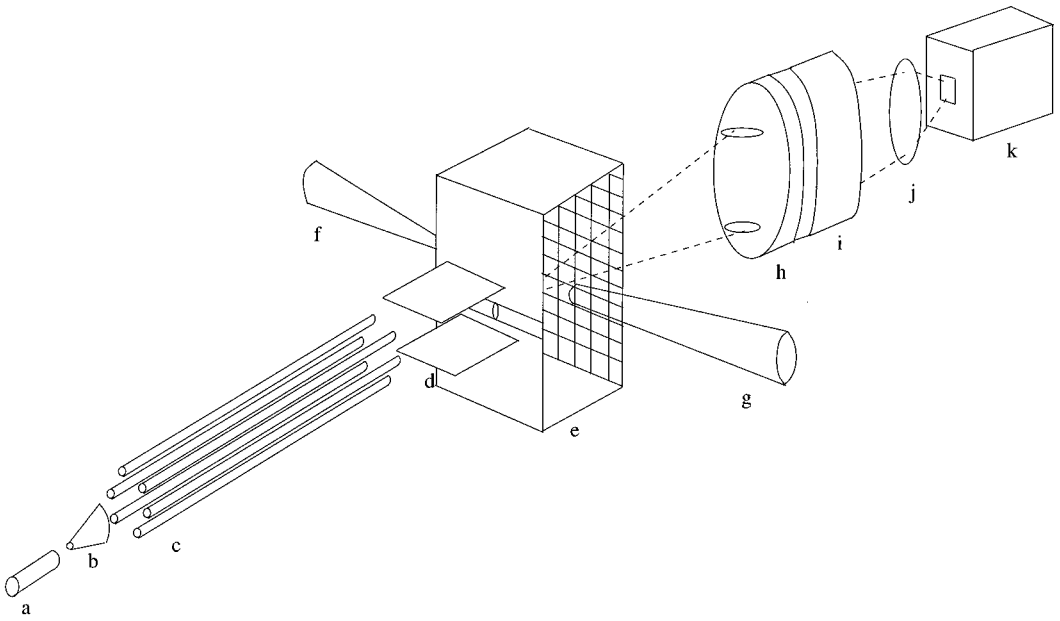

Figure 1. Schematic view of the imaging machine. Note that the different parts are not drawn to scale: (a) pulsed nozzle, (b) skimmer, (c) hexapole, (d) guiding field electrodes, (e) orientation field electrodes, (f) REMPI laser (probe laser), (g) dissociation laser, (h) microchannel plate, (i) phosphor screen with vacuum fibered window, (j) camera lens to image fluorescence, and (k) cooled CCD camera (or photomultiplier).

iodide. By combining hexapole state selection with ion imaging detection methods, we can image state-specific angular distributions of photofragments from oriented molecules. First results for the simple photodissociation of oriented methyl iodide (CD_3I) at 266 nm have been reported;[26] however, these results were obtained for rather low orientation field strength. Experimental improvements have opened the possibilities of applying much stronger orientation fields.

With the combination of state selection and photofragment imaging, it is possible to study in complete detail the photolysis of a single quantum state. Imaging of half and full collision processes is rapidly developing as an extremely powerful technique for elucidating the detailed dynamics of inelastic and reactive collisions.[25] Using the technique of electric hexapole state selection, it is possible to create essentially single-state beams of symmetric top molecules which can be oriented in space. With these hexapole state-selected parent beams one can also study details of the dissociation dynamics as reflected in the rotational state distribution of fragments and the effect of the initially selected quantum state of the parent molecule.[26,27]

The experiments described here extend the measurements reported before[26] and give a detailed analysis of the dependence of the observed recoil distribution as a function of the electric field strength used to orient the parent molecules. A description of the apparatus is given in section 2. In section 3 we present the recoil distribution of the $I(^2P_{1/2})$ fragment channel (I*) obtained from the dissociation of methyl iodide, CD_3I, at 266 nm. Methyl iodide is an obvious choice for demonstrating the capabilities of the oriented molecule imaging method, since the photolysis has been extensively studied by other methods. Bernstein and co-workers used the time-of-flight arrival spectrum of I* photofragments from dissociation of state-selected and oriented CH_3I to obtain the forward−backward degree of orientation of the parent molecules.[17,18] We will analyze the orientation field strength dependence of the measured recoil distribution and discuss the effect of the hyperfine interaction on the prepared orientation distribution of the parent molecule. In section 4 we will discuss our results, and we will summarize our conclusions in section 5.

2. Experimental Section

The experiments described here use a newly constructed apparatus which allows final state-, velocity-, and angle-resolved detection of fragments from the photodissociation of oriented molecules prepared in a single quantum state. A schematic view is given in Figure 1. In this section we will first describe and discuss the state selection of the parent molecules (section 2.1). In section 2.2 we will describe the way the state-selected molecules are oriented and the photofragments are imaged onto the two-dimensional detector. Note that the parts in Figure 1 are not drawn to scale; *e.g.* the length of the hexapole (part c in Figure 1) is 1 m, and the distance between the two main orientation plates (part e in figure 1) is 2.6 cm only.

2.1. State-Selection. A cold pulsed molecular beam is created by expansion of typically a 5% mixture of CD_3I in Kr with a pulsed nozzle (General Valve; orifice diameter, 0.3 mm). The source chamber is pumped by a diffusion pump (pumping speed, 11.000 L/s) backed by a roots pump and a motor pump. The beam is skimmed about 5 cm downstream (skimmer diameter, 1.5 mm) and enters a second chamber, the buffer chamber, which is pumped by a small turbo pump. In this chamber an additional beam chopper can be mounted to slice out part of the gas pulse. In the experiments reported here the chopper was taken out of the beam. The buffer chamber is seperated from the third chamber by a fixed diaphragm (diameter, about 15 mm). The third chamber contains a 1 m long hexapole. The diameter of the rods is 4 mm. The hexapole can be positioned and aligned from outside in order to optimize the focusing of the state-selected molecules onto a small hole (about 1.5 mm diameter) in the orientation/repellor fields (see Figure 1). The distance from the nozzle to the entrance of the hexapole is 30 cm. The distance from the exit of the hexapole to the center of the imaging chamber where the pulsed beam is crossed with the lasers is 21 cm.

For a description of the charateristics of hexapole state selectors, we refer to the extensive literature on this (see *e.g.* ref 28 and references cited therein). In short, symmetric top like molecules traveling through the inhomogeneous electric field of the hexapole follow sinusoidal trajectories and focus at a certain point, depending on their rotational quantum numbers

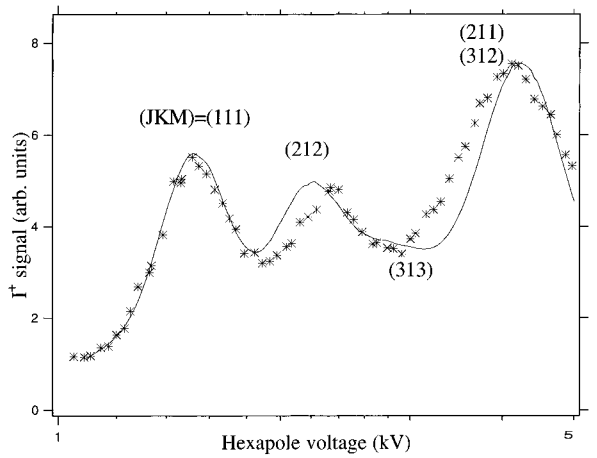

Figure 2. Experimental (asterisks) and simulated hexapole transmission curves. For the simulated curve rotational temperatures of $T_J = 3.3$ K and $T_K = 5.8$ K were used, the average beam velocity was 425 m/s, and the speed ratio (S) was 12. The total light yield from the phosphor screen was collected by replacing the CCD camera with a photomultiplier.

(JKM) and the voltages on the hexapole rods. Here J is the total rotational angular momentum of the molecule, K is the projection of the angular momentum on the figure axis of the molecule, and M is the projection of the angular momentum on the direction of the externally applied (dc) electric field.

In a cold molecular beam there will be only one or two rotational states populated that have the same $MK/J(J + 1)$ value. By selecting a proper hexapole voltage molecules in a chosen (JKM) rotational state will be focused on the entrance to the interaction region with the lasers. When the voltage on the hexapole is scanned and the total beam intensity is measured, we obtain the so-called focusing spectrum (see Figure 2). In Figure 2 the yield of I($^2P_{1/2}$) atoms from the dissociation of CD_3I is shown as a function of the voltage on the hexapole. The total ion yield was measured by replacing the two-dimensional detector by a photomultiplier tube (see section 2.2). Several peaks can be observed in the focusing spectrum, and they can be identified with certain rotational states (JKM) as indicated near the peaks. The solid curve in Figure 2 is a simulation of the hexapole focusing curve of CD_3I using the first-order Stark effect only. The rotational temperature of our beam is found to be about 3 K. For our seeding and focusing conditions the typical increase of the intensity of the state-selected beam relative to the direct beam (hexapole voltage off) is about a factor of 4−5 for (JKM) = (111).

2.2. Orientation and Imaging. In order to preserve the M selection of the state-selected beam from the exit of the hexapole to the interaction region with the photolysis laser, an electric field can be applied to guide molecules from the hexapole to the photodissociation region. This is the so-called guiding field (indicated by part d in Figure 1) and consists of two capacitor-like plates spaced 10 mm apart. In the interaction region a strong vertically directed electric field can be applied to orient the parent molecules (see the upper panel at time $T = 0$ in Figure 3). The ion-repeller plate is also split in two so that a vertical field is preserved for the molecules going from the guiding field zone to the laser interaction zone. We have simulated our electrode geometry to study how strong and homogeneous the field is at the dissociation region. Because we have an ion extraction grid present (the gridded structure in Figure 3), the actual field strength is somewhat less than is expected from a simple capacitor field. When the orientation field is present, this extraction grid is maintained at 0 V. The simulation (SIMION software) shows that the field is weaker by a factor

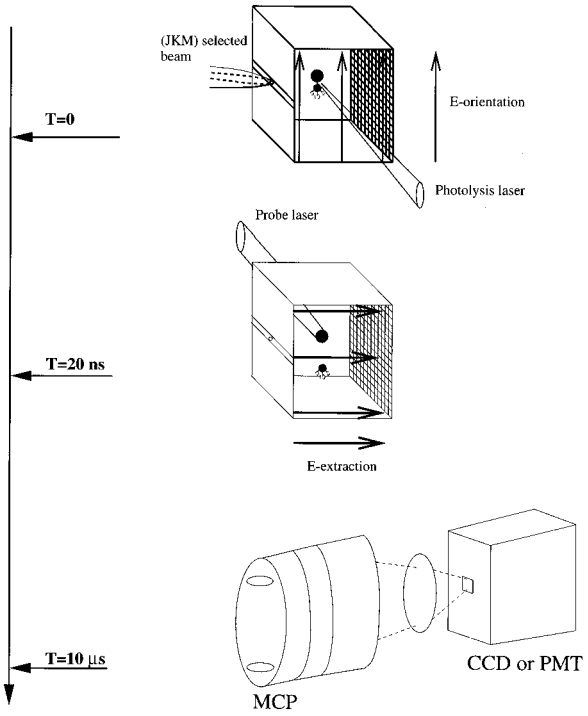

Figure 3. Schematic of the experimental time sequence. The oriented molecules are photodissociated by a first laser pulse at time $T = 0$; then the electric fields are switched from the vertical orientation direction to the horizontal extraction direction. At time $T = 20$ ns the fragments are ionized with a probe second laser pulse. The ions are accelerated and enter a time-of-flight tube, at the end of which they encounter the MCP. The front plate of the MCP is gated when the ions of appropriate mass arrive.

0.83. This means that the experimental field strength used to orient the parent molecules was calculated as 0.83(V-or)/2.6 V/cm, where V-or is the sum of the applied positive and negative voltages on the two main orientation plates.

Because we need to extract the fragment ions in a direction perpendicular to the orientation direction, we have to change the field direction. In order to do this we use several fast high-voltage transistor switches (Behlke, Germany) to change in several tens of nanoseconds the voltage applied on the various orientation and extraction fields. To damp the overshoot and the ringing of the voltage on the various plates when they are rapidly switched, a small resistor was put in series, compromising somewhat on the speed of the switching. Typically, switching times of about 20−30 ns are obtained.

After the electric field is switched from orientation field to ion extraction field, the probe laser is fired to ionize one of the photolysis fragments. The ionization process does not effect the recoil velocity of the photofragment because of the small mass of the ejected electron. The ions are accelerated into a short time-of-flight tube (17 cm length). When the ion of interest arrives at the microchannel plate (MCP, Galileo dual Chevron type with 42 mm effective diameter), the front plate is switched from 0 V up to −1000 V. This turns on the gain on the MCP. The second plate of the MCP always has a voltage applied. In this way, the detector can be used to measure only the position of the ions of interest and the detection of unwanted background can be suppressed. The electrons at the back of the MCP are accelerated onto a fast phosphor screen (P47, lifetime about 80 ns) and the fluorescence is imaged with a high-quality camera lens (Nikon, $f = 35$ mm, 1.4) onto a charge-coupled-device (CCD) camera. The CCD camera (Princeton Instruments) is equiped with a 512 × 512 pixels, back-illuminated Tektronix chip in multipin-phasing (MPP) mode and

thermoelectrically cooled to about −50 °C. The quantum efficiency of this back-illuminated chip is about 60% at 400 nm, which is the peak wavelength of the P47 phosphorescence. The CCD camera is operated in the so-called slow-scan mode, which means that the shutter is opened for a set time to integrate on chip the light from the phosphor screen. The typical dark charge is less than 1 electron/(pixel·s). The readout noise of the A/D converter (14 bits) is about 5 electrons, which is set to one count. After this integration period (typically up to 5 min), the shutter is closed, the camera is read-out, and the image is stored on a PC (486/33). When the total ion signal is wanted, the CCD camera is replaced by a photomultiplier tube.

The dissociation laser used in these experiments is the fourth harmonic of a YAG laser (repetition rate, 10 Hz), and the typical photolysis energy used is about 1−3 mJ/pulse. The probe laser is the doubled output from a YAG pumped dye laser (Spectra Physics PDL3), and probe pulse energies of about 1.5 mJ were used. The photolysis laser was typically focused with a $f = 15$ cm lens; for the probe laser we used a $f = 20$ cm lens. The polarization of the photolysis laser was parallel to the vertical direction of the orientation field, and in most cases the polarization of the probe laser was also set vertically unless stated otherwise.

3. Results

3.1. Imaging of Photofragments. In this section we report on the imaging of $I(^2P_{1/2})$ photofragments from the dissociation of CD_3I at 266 nm. The $I(^2P_{1/2})$ fragments were detected by (2 + 1) resonance-enhanced multiphoton ionization (REMPI) around 305 nm. The images reported here were all taken with an exposure time of 5 min, resulting in an accumulation of 3000 laser shots. After measurement of a state-selected and oriented image a background image was taken with the same exposure time. The background image was taken under exactly the same experimental conditions as the oriented image but with zero voltage on the hexapole rods. In this way we obtain the contribution of nonoriented molecules to the state-selected images. The intensity of the direct beam image is typically less than 20% of the intensity of the state-selected (JKM) = (111) image; see also the focusing curve of Figure 2.

In Figure 4 three images (a−c) are shown, which were obtained by subtraction of the background image from the state-selected image. The images shown are 226 pixels long vertically and 200 pixels wide horizontally. The raw background subtracted images were convolved with a Gaussian mask of 5 × 5 pixels, and each line of data was left−right averaged because the Abel inversion (see below) needs a symmetric line of data.

The images were taken at three different orientation field strengths: (a) $E = 0$V/cm, (b) $E = 96$ V/cm, and (c) $E = 1.6$ kV/cm. The direction of the polarization of the photolysis laser was parallel to the vertical direction of the orientation field. Because the (JKM) state-selected parent molecules have a positive Stark energy, the negative end of the methyl iodide molecules (I end) is directed toward the negatively charged orientation electrode. This was the upper electrode for the oriented images shown in Figure 4. The actual field strength was calculated from simulations of the field geometry in our setup (see section 2.2). The hexapole voltage was set at the value corresponding with the focusing voltage for the (JKM) = (111) state. The images of Figure 4 represent the two-dimensional projection of the angular recoil distribution of I* fragments onto the two-dimensional detector plane. This plane is parallel to the direction of the DC electric field that orients the parent molecule CD_3I in (JKM) = (111). The photofragment

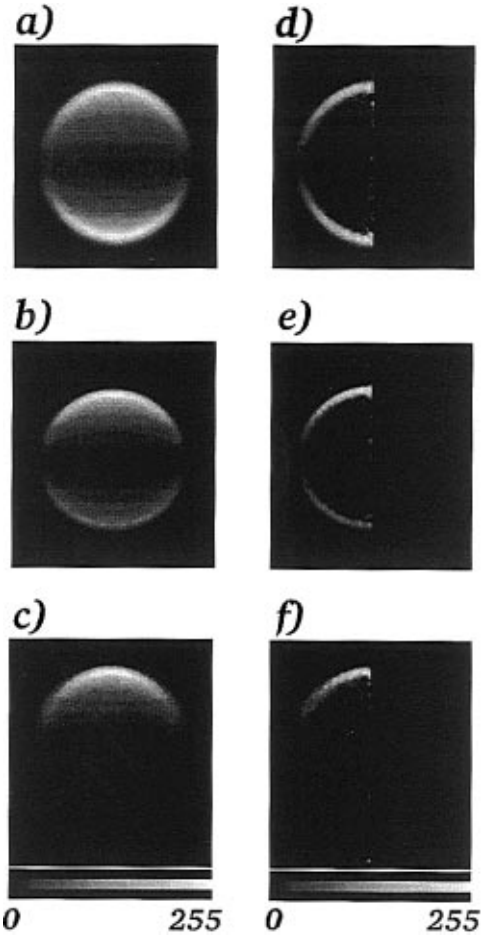

Figure 4. Two-dimensional images of the recoil distribution of I* fragments from the photodissociation at 266 nm of state-selected and oriented (JKM) = (111) CD_3I parent molecules. The orientation field was directed along the vertical direction (parallel to the linear polarization of the dissociation laser; see Figure 3) with the parent molecule oriented with the I end of the molecule in the upward direction. In image a no orientation field was present, in image b the orientation field was 96 V/cm, and in image c it is 1600 V/cm. Images d−f are the Abel-inverted images of the two-dimensional data of images a−c, respectively. Note that the Abel-inverted images are a cut trough the cylindrically symmetric three-dimensional distribution and can be rotated around the vertical axis. Therefore the right half of the Abel-inverted image is shown in black. The grey scale bar at the bottom corresponds to a linear intensity scale with black = 0 and white = 255.

angular intensity is represented by a grey scale indicated by the bar below, where minimum intensity corresponds with black and maximum intensity corresponds with white. The intensity in each image is scaled to the maximum intensity which is set to 255.

The zero field image (Figure 4a) was obtained by maintaining a constant ion acceleration field and having no guiding or orientation field present. The recoil distribution shows two projected polar caps along the direction of the polarization of the photolysis laser, which is very characteristic of a parallel type of transition. When we apply an orientation field (panels b and c) in the photolysis region, the state-selected CD_3I parent molecules become (partially) oriented with the iodine, pointing predominantly in the upward vertical direction. The images clearly show the asymmetry in the recoil distribution. At 266 nm the absorption is a parallel transition, and the dissociation is prompt (<100 fs) and axial. This means that the I* fragments are ejected in the direction of the figure axis of the parent molecule at the moment of the photoabsorption.

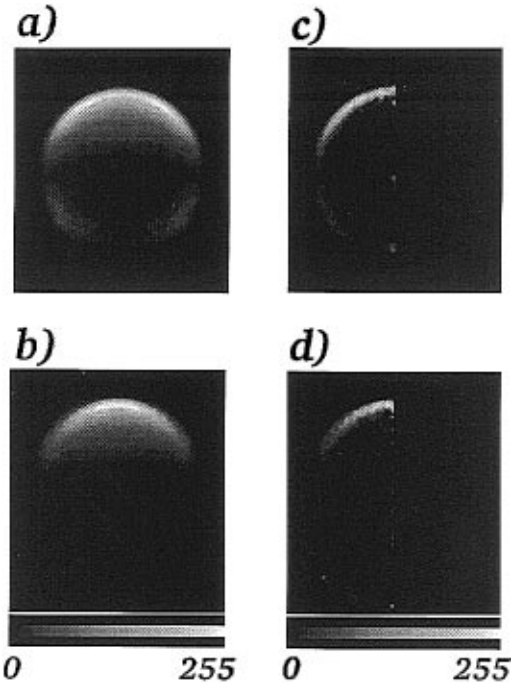

Figure 5. Two-dimensional images of the recoil distribution of I* from dissociation of state-selected CD_3I molecules in (a) $(JKM) = (212)$ and (b) $(JKM) = (111)$. The orientation field strength was 1600 V/cm. Panels c and d are the Abel-inverted images. See also the caption of Figure 4.

The three-dimensional recoil distribution of fragments is cylindrically symmetric around the direction of the polarization of the dissociation laser and is projected onto the two-dimensional plane of the MCP detector. This projection is perpendicular to the symmetry axis of the original three-dimensional distribution which makes it possible to reconstruct the three-dimensional distribution of recoiling fragments via a mathematical process called Abel inversion.[29] The resulting Abel-inverted images are shown in panels d−f of Figure 4 corresponding to the two-dimensional data of panels a−c, respectively. From the three-dimensional inverted image we can obtain the recoil intensity as a function of the angle θ between the space-fixed direction of the dc orientation field and the recoil direction. Because the dissociation is very fast and axial, the recoil distribution of photofragments reflects the initial orientational distribution of the parent molecule. This will be discussed in more detail and more quantitatively in section 4.

To illustrate this further, we measured the recoil distribution of $(JKM) = (212)$ state-selected and oriented molecules. The hexapole was set at a voltage of about 2.5 kV, selecting mainly parent molecules with $(JKM) = (212)$; see Figure 2. The resulting image (with similar background subtraction, convolution, and averaging left−right) is shown in Figure 5, panel a, and compared with the image of the $(JKM) = (111)$ state in panel b. The orientation field strength used was in both cases the same, 1.6 kV/cm. As can be clearly observed in Figure 5, the recoil distribution of panel a is wider than the distribution of panel b. The wider distribution and the shift of the maximum intensity away from the vertical axis reflects the initially prepared orientational distribution of the $(JKM) = (212)$ parent molecule, as will be discussed in more detail in section 4. In panels c and d the corresponding Abel-inverted images of the images of panels a and b are shown.

3.2. The Rotational Product State Distribution. We have measured the rotational product state distribution of the CD_3 fragment from photolysis at 266 nm using the $3p_z \leftarrow \tilde{X}\ 0_0^0$ two-photon resonant transition as the intermediate in the $(2 + 1)$ ionization process. The hexapole voltage was set to select CD_3I parent molecules in $(JK) = (11)$. We did not apply an orientation field in this experiment, so we have randomly oriented parents. The measured spectrum, with the polarization of the probe laser at the magic angle (54°) with respect to the dissociation laser, is shown in panel a of Figure 6. A simulation of the spectrum, using a line-by-line analysis, similar to the procedure reported before,[30] is shown in panel b of Figure 6. A comparison of the experimental spectrum of the state-selected parent with the cold but non-state-selected parent (see Figure 2 of ref 30) immediately reveals the absence of the alternation of the peak intensity on the O and S branches with even−odd rotational quantum number N. These branches probe the $K = 0$ levels in the CD_3 fragment, and they have a strong alternation of the nuclear statistical weight with even−odd N. In Figure 7 we show the populations used for our simulation (panel a), and we compare them with the populations obtained for the non-state-selected parent of refs 30 and 31. It is found that rotational levels (N,K) with $K = 1$ are populated most dominantly. If we sum the populations over the rotational levels N at fixed K, we observe from our simulation that about 11% is in $K = 0$, 68% is in $K = 1$, 16% is in $K = 2$, and 5% in $K = 3$. This means that overall the average K in the CD_3 fragment is about 1.15 and the predominant propensity is for conservation of the helicity quantum number K from the excited parent CD_3I to the CD_3 fragment. From our simulations it appears that we do get some

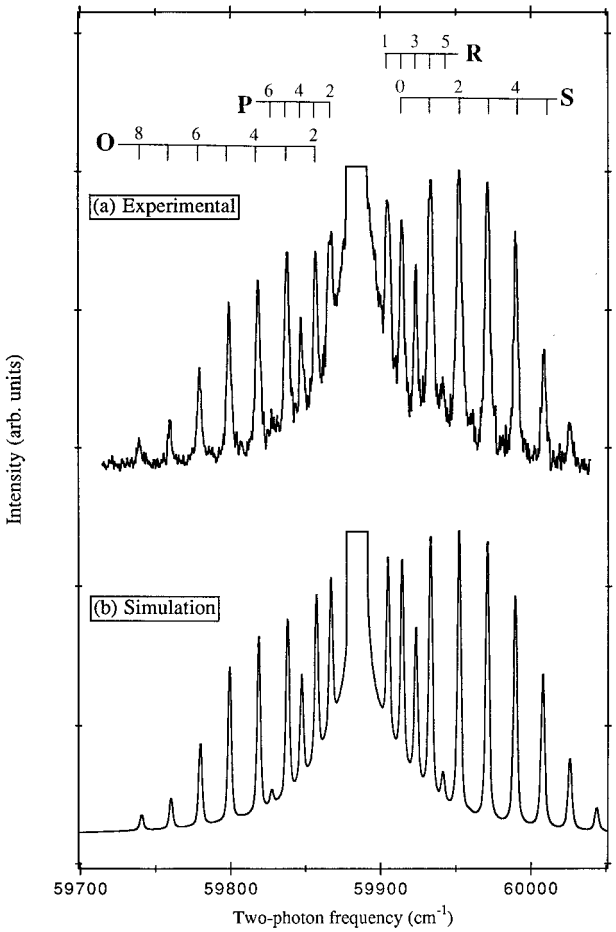

Figure 6. REMPI spectrum of the $3p_z \leftarrow \tilde{X}\ 0_0^0$ band of CD_3 from dissociation of $(JK) = (11)$-selected CD_3I parents. The very strong Q-branch was clipped in the figure. Panel b shows a simulation using the populations of Figure 7. The simulation was done on a line-by-line analysis as described before in ref 30. The effect of predissociation on the Lorentzian line shape was accounted for using a homogeneous line width of 1.0 cm^{-1} and a heterogeneous line width parameter of 0.0095 cm^{-1}.

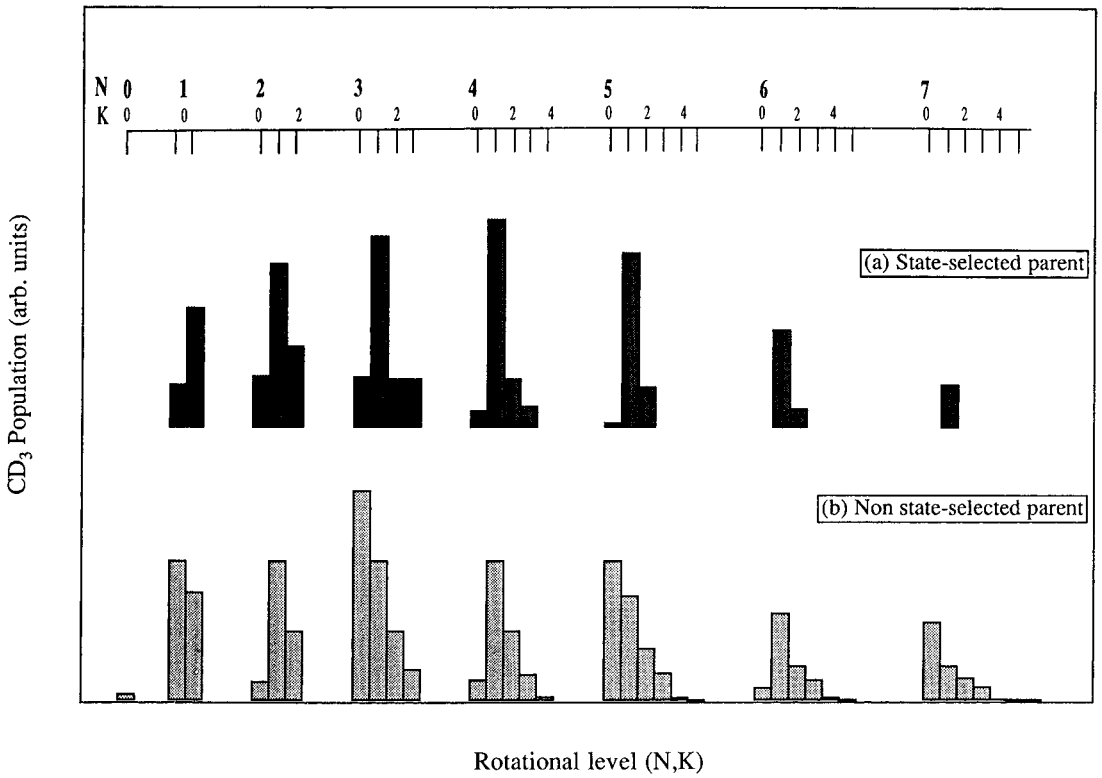

Figure 7. Comparison of the extracted populations from the simulation of the REMPI spectra of state-selected parent (this work) and non-state-selected parent.[30,31]

minor population in $K = 2$ and $K = 3$ states. Baugh and co-workers[27] have also reported rotational product state distributions in CD_3 from photolysis of $(JK) = (11)$ state-selected CD_3I parent molecules. In their setup the $K = 1$ purity of state selection was estimated to be about 94%, which is somewhat better than in our experiment. We have a much shorter hexapole (1 m versus 3.8 m), and from our focusing spectrum we find that the intensity of the direct beam (containing all K states) is about a factor of 4−5 smaller than the $(JKM) = (111)$ selected beam. Therefore, in our spectral simulation we did include $K = 0$ population, contrary to the analysis of ref 27. It was argued in ref 27 that the observed $\Delta K = 3$ transitions were due to nonadiabatic coupling in the region of the conical intersection of the $^3Q_0$ and $^1Q_1$ surfaces. So far, the most extensive theoretical calculations of the rotational product state distribution[32−34] reported do not give quantitative numbers for the total amount of rotational excitation parallel to the C_3 axis, but merely state that this is exceedingly small.[33] In all of the calculations it is assumed that the parent starts in the rotationless state $J = 0$. In the state-selected experiments the initial state is $(JK) = (11)$, and this may affect somewhat the product state distribution. At this point we can only conclude that the overall rotational distribution is in agreement with the measurements of Baugh and co-workers and theoretical calculations. A more quantitative comparison with the $\Delta K \neq 0$ transitions awaits further theoretical calculations.

4. Discussion

In this section we want to examine more quantitatively the information which can be obtainend from the recoil distribution of the images presented in section 3. As was discussed before by Taatjes *et al.*,[7] in general more information about the dissociation dynamics can be obtained when oriented parent molecules are used. The dissociation of methyl iodide at 266 nm has been studied very extensively, both theoretically and experimentally. For a recent overview of references we like to refer to the extensive list of references on the A-band photodissociation in methyl iodide in the paper by Amatatsu *et al.*[34] It is generally observed that the dissociation is very fast and the dissociation channel $I(^2P_{1/2})$ + methyl CD_3 produces little rotational excitation. This all indicates a rather isotropic surface which is confirmed by *ab initio* calculations by Morokuma and co-workers.[35] For excitation at 266 nm the important potential surfaces involved are the A_1 ($^3Q_0$) and E ($^1Q_1$) states in symmetric C_{3v} symmetry which give rise to A′ and A′ + A″ surfaces at a bent geometry. These calculations show that, at the crossing of the $^3Q_0$ surface to which the excitation takes place and the $^1Q_1$ surface, the A′ surface which correlates with the I* channel has only a small energy difference between the linear geometry and the energy minimum, which is at a bent angle of about 4.4°. Beyond the crossing point of the surfaces, the upper A′ surface has a minimum at linear geometry and is stronger curved than the lower A′ surface. Therefore, any bending away from linear geometry induced at the curve crossing will be forced back toward linear geometry, and the I* fragment is expected to be ejected along the initial direction of the molecular symmetry axis of the parent.

In order to compare our observed recoil distributions of parent molecules in $(JKM) = (111)$ states, as presented for three different orientation voltages in Figure 8, we calculated the expected recoil distribution. The laboratory-frame axis probability density distribution of the state-selected parent molecule, I_{axis}, can be described by (see *e.g.* refs 5 and 10)

$$I_{axis}(\cos\theta) = c_0P_0(\cos\theta) + c_1P_1(\cos\theta) + c_2P_2(\cos\theta) \quad (1)$$

where $P_i(\cos\theta)$ are the Legendre polynominals and c_i the weighting coefficients. In case of an isotropic distribution $c_0 = {}^1/_2$ and $c_1 = c_2 = 0$; in case of a fully oriented $(JKM) = (111)$ state $c_0 = {}^1/_2$, $c_1 = {}^3/_4$, and $c_2 = {}^1/_4$. In the case of methyl iodide strong hyperfine interactions cause a reduction of the maximum obtainable axis orientation at low to moderate

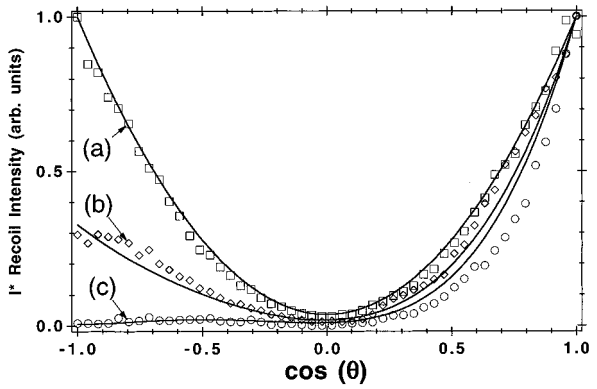

Figure 8. Recoil distributions of I* fragments from dissociation of (*JKM*) = (111) state-selected and oriented CD_3I parents at different orientation field strengths. The distributions were obtained from the Abel-inverted images d−f of Figure 4. The solid lines are the expected theoretical curves for a prompt axial recoil in the molecular frame with $\beta = 1.8$ (see text).

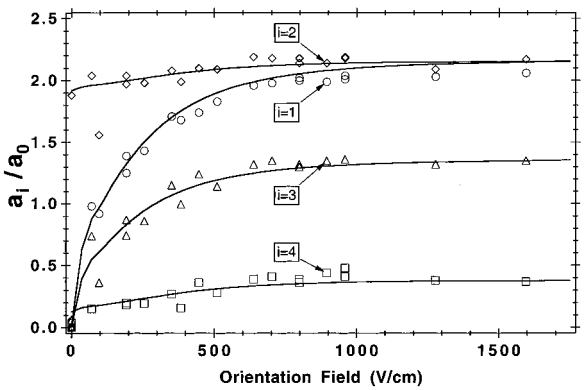

Figure 9. Extracted expansion coefficients a_i/a_0 ($i = 1-4$) of the different Legendre contributions to the recoil distribution of I* from the Abel-inverted images. The solid curves are the theoretically expected values obtained from Stark effect calculations (see text).

orientation fields. Extensive calculations have been done by Bulthuis *et al.*[36,37] on the Stark effect in CH_3I. We have used their distribution coefficients to calculate the axis distribution for CD_3I. We do not expect that the deuterated methyl iodide will have much different weigthing coeffcients because the main contribution to the hyperfine interaction is due to the I atom. The solid curves in Figure 8 represent the recoil distribution of photofragments, $I_{recoil}(\cos\theta)$, in the limit of a prompt and axial recoil and were calculated as

$$I_{recoil}(\cos\theta) = I_{axis}(\cos\theta)(1 + \beta P_2(\cos\theta)) \qquad (2)$$

Overall we get a good agreement with the experimental results when we use $\beta = 1.8$. In the past several experiments have been reported on the β parameter of the I* channel of photodissociation of methyl iodide at 266 nm, and they range between 1.8 and 2.0.[39,40,41,42]

Another more quantitative comparison can be made by extracting the Legendre moments of the experimental recoil distribution I_{recoil}. It is

$$I_{recoil}(\cos\theta) = \sum_{i=0}^{n} a_i P_i(\cos\theta) \qquad (3)$$

As can be seen from eq 2, we can extract moments up to $i = 4$ because the axis distribution $I_{axis}(\cos\theta)$ for a (*JKM*) = (111) state is specified by a Legendre expansion up to $i = 2$. We can write explicitly

$$a_1/a_0 = \frac{c_1 + {}^2/_5\beta c_1}{c_0 + {}^1/_5\beta c_2} \qquad (4)$$

$$a_2/a_0 = \frac{c_2 + \beta c_0 + {}^2/_7\beta c_2}{c_0 + {}^1/_5\beta c_2} \qquad (5)$$

$$a_3/a_0 = \frac{{}^3/_5\beta c_1}{c_0 + {}^1/_5\beta c_2} \qquad (6)$$

$$a_4/a_0 = \frac{{}^{18}/_{35}\beta c_2}{c_0 + {}^1/_5\beta c_2} \qquad (7)$$

In Figure 9 we compare the extracted experimental moments a_i/a_0 with the theoretically calculated moments, using the field-dependent coefficients c_1/c_0, c_2/c_0 from the Stark effect calculations.[36,37] Again we used $\beta = 1.8$ to calculate the theoretical moments using eqs 4−7. The experimental moments follow quite well the field dependence of the calculated moments, indicating that the extracted angular distribution of photofragments can be used in principle to obtain quantitative information beyond the β-parameter only. Baugh and co-workers[19,38] described how from measurement of the differential cross-section of *m*-state-specific photofragments from the dissociation of oriented or aligned parent molecules information about the phases and magnitudes of the transition dipole matrix can be obtained. Assuming a parallel excitation and zero angular momentum for the nondetected co-fragment, they discuss the relation between the measured moments of the product density matrix describing the photodissociation and the transition dipole matrix. A first attempt to extract quantitative transition dipole matrix elements assuming these conditions was reported for the dissociation of oriented CD_3I.[19]

A few years ago Bernstein and co-workers[18] reported an experimental study on the orientation field dependence of the molecular orientation in CH_3I using a TOF detection method. From their TOF data they extracted their so-called κ parameter. This κ parameter describes the ratio of the intensity of I* photofragments measured in the lower hemisphere (*i.e.* with cos $\theta < 0$) to that in the upper hemisphere ($\cos\theta > 0$). A more quantitative analysis of the extracted κ values and their field dependence[36] showed that there was a discrepancy with the theoretically expected κ. It was noted[18] that experimental difficulties in properly discriminating the intensities in the upper and lower hemisphere out of the TOF data was the main source for a quantitative comparison of the molecular orientation at high field strength. In ref 36 a somewhat arbitrary background correction was done to bring these corrected κ values in agreement with the theoretically calculated values.

From our Abel-inverted three-dimensional intensity distribution we can also integrate the intensity of the lower and upper hemisphere and compare these values with the result of the TOF method and the theoretical values. This is shown in Figure 10. As is seen from the comparison the κ values obtained from the imaging data follow very closely the theoretically expected field strength dependence and are in much better agreement than the values from the TOF experiments. Only at very high voltage there appears to be a small difference, but it should be noted that for these high voltages the intensity in the lower hemisphere is very low. The noise generated by the Abel inversion may introduce here some artificial intensity.

In Figure 5 we showed two images for CD_3I parents starting in different initial states, (*JKM*) = (111) versus (212). The

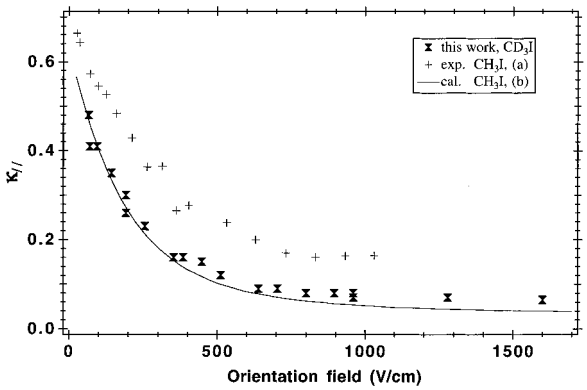

Figure 10. Comparison of the measured lower−upper hemisphere intensity ratio κ from the recoil distribution of the measured images as a function of the orientation field strength, with (a) the experimental time-of-flight data of Bernstein and co-workers[18] for CH_3I and the (b) theoretically expected values for CH_3I as calculated by Bulthuis *et al.*[37]

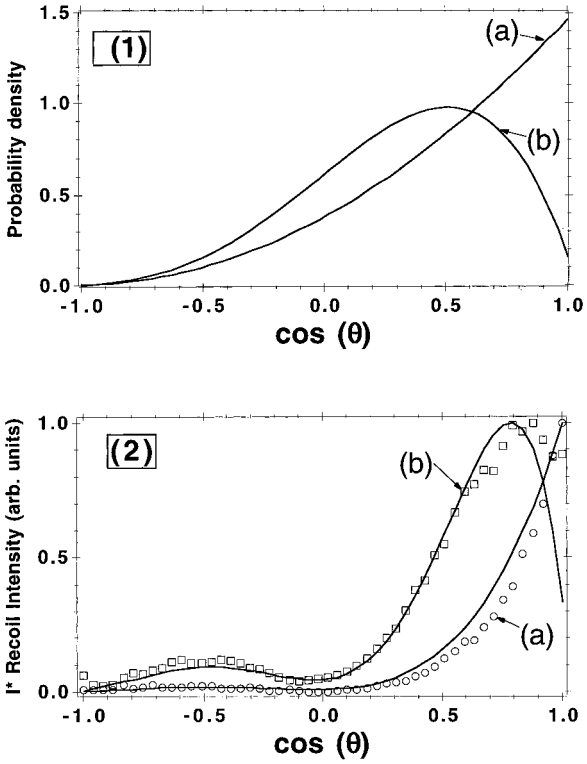

Figure 11. In panel 1 a comparison of the axis density distribution of oriented CD_3I at an orientation field of 1600 V/cm for two different initial states (a) (*JKM*) = (111) and (b) (*JKM*) = (212). In panel 2 the measured fragment recoil distribution of I* fragments from dissociation of state-selected and oriented CD_3I parents in two different quantum states, (*JKM*) = (111) and (*JKM*) = (212). The solid curves are the theoretically expected curves for a prompt axial recoil with $\beta = 1.8$ and the axis distributions of panel 1.

difference in the observed recoil distribution of I* fragments can be ascribed to the different axis-probability density of these oriented states. In Figure 11, panel 1, we compare the two densities which are calculated from the Stark effect calculations[37] at an orientation field strength of 1600 V/cm. The (*JKM*) = (212) state at this voltage has not yet fully developed to the maximum obtainable orientation for a (212) state which should have zero probability density for $\cos\theta = 0$. Furthermore, the (212) density is larger for angles $\theta \geq 90°$ than the (*JKM*) = (111) density.

To compare the recoil distributions more quantitatively, we show in Figure 11, panel 2, the two measured distributions and the theoretically expected distributions for $\beta = 1.8$ using the axis distributions of panel 1 and eq 2. We observe a quite satisfactory agreement, although for $\cos\theta = 0$ the measured intensity is somewhat larger. Maybe one reason for this is that when we set our hexapole voltage at the peak corresponding to the (212) peak, we still focus (although with much less intensity) some parent molecules in (*JKM*) = (111). These will contribute in the recoil distribution mostly at $\cos\theta = 0$, causing deviations with the distribution from a (212) parent only. Another reason may be some experimental smearing effects caused by an extended source of photofragments due to the finite width of the molecular beam.

Overall we observe a direct reflection of the spatial orientation distribution of the parent molecule in the spatial recoil distribution of the $I(^2P_{1/2})$ photofragments for this rapid and axial dissociation of methyl iodide at 266 nm.

5. Conclusions

In this paper we have reported on the two-dimensional imaging of the recoil distribution of I* photofragments from the dissociation at 266 nm of (*JKM*) state-selected and oriented parent molecules. The images reflect the spatial degree of orientation of the parent state. At high orientation fields the extracted orientation distribution for dissociation of CD_3I in (*JKM*) = (111) agrees very well with a fully oriented (*JKM*) = (111) distribution. The imaging method allows one to obtain the full three-dimensional recoil distribution of photofragments from which more details can be obtained compared to the TOF experiments reported before. Methyl iodide has proven to be a good benchmark molecule for assessing the quantitative degree of information about the orientation distribution of the parent state which can be obtained from imaging photofragments from hexapole-oriented parent molecules. In the future we will report on photodissociation studies of molecules like N_2O and CH_3Br in which the dynamics is more complicated due to interacting excited state surfaces and stronger anisotropic forces. This will result in a deviation of the recoil of fragments from the initial orientation of the bond axis. Imaging of fragments from state-selected and oriented molecules in these systems is expected to provide more intimate information about the dissociation dynamics.

Acknowledgment. The authors would like to thank Dr. D. W. Chandler for help and technical advice about imaging and providing the software programs for the Abel inversion, Dr. C. A. Taatjes for many helpful discussions and encouragement, and Dr. J. Bulthuis for discussions about the hyperfine effect and providing the numerical Legendre moments of oriented wave functions of CH_3I. We would like to thank Mr. K. Nauta for his help in setting up the Khoros analysis software. The Netherlands Organization for Scientific Research (NWO) is gratefully acknowledged for financial support through SON and FOM. The research of M.H.M.J. has been made possible by a fellowship of the Royal Netherlands Academy of Arts and Sciences (KNAW).

References and Notes

(1) Zare, R. N. *Mol. Photochem.* **1972**, *4*, 1.
(2) Yang, S.; Bersohn, R. *J. Chem. Phys.* **1974**, *61*, 4400.
(3) Jonah, C. *J. Chem. Phys.* **1971**, *55*, 1915.
(4) Busch, G. E.; Wilson, K. R. *J. Chem. Phys.* **1972**, *56*, 3638.
(5) Choi, S. E.; Bernstein, R. B. *J. Chem. Phys.* **1986**, *85*, 150.
(6) Zare, R. N. *Chem. Phys. Lett.* **1989**, *156*, 1.
(7) Taatjes, C. A.; Janssen, M. H. M.; Stolte, S. *Chem. Phys. Lett.* **1993**, *203*, 363.
(8) Seideman, T. *J. Chem. Phys.* **1995**, *102*, 6487.
(9) Seideman, T. *Chem. Phys. Lett.* **1996**, *253*, 279.
(10) Stolte, S. *Ber. Bunsen-Ges. Phys. Chem.* **1982**, *86*, 413.

(11) Loesch, H. J.; Remscheid, A. *J. Chem. Phys.* **1990**, *93*, 4779.
(12) Friedrich, B.; Herschbach, D. R. *Nature (London)* **1991**, *353*, 412.
(13) Jalink, H.; Janssen, M.; Harren, F.; van den Ende, D.; Meiwes-Broer, K.-H.; Parker, D. H.; Stolte, S. In *Recent Advances in Molecular Reaction Dynamics*; Vetter, R., Vigué, J., Eds.; CNRS: Paris, 1986; p 41.
(14) Gandhi, S. R.; Bernstein, R. B. *J. Chem. Phys.* **1987**, *87*, 6457.
(15) Parker, D. H.; Jalink, H.; Stolte, S. *J. Phys. Chem.* **1987**, *91*, 5427.
(16) Janssen, M. H. M.; Parker, D. H.; Stolte, S. *J. Phys. Chem.* **1991**, *85*, 5372.
(17) Gandhi, S. R.; Curtiss, T. J.; Bernstein, R. B. *Phys. Rev. Lett.* **1987**, *59*, 2951.
(18) Gandhi, S. R.; Bernstein, R. B. *J. Chem. Phys.* **1990**, *93*, 4024.
(19) Pipes, L. C.; Kim, D. Y.; Brandstater, N.; Fuglesang, C. D.; Baugh, D. *Chem. Phys. Lett.* **1995**, *247*, 564.
(20) Torres, E. A.; Kim, D. Y; Pipes, L. C.; Baugh, D. A.; Seideman, T. *J. Chem. Soc., Faraday Trans.* **1997**, *93*, 931.
(21) Ohoyama, H.; Ogawa, T.; Makita, H.; Kasai, T.; Kuwata, K. *J. Phys. Chem.* **1996**, *100*, 4729.
(22) Volkmer, M.; Meier, Ch.; Lieschke, J.; Mihill, A.; Fink, M.; Böwering, N. *Phys. Rev. A* **1996**, *53*, 1457.
(23) Wu, M.; Bemish, J.; Miller, R. E. *J. Chem. Phys.* **1994**, *101*, 9447.
(24) Chandler, D. W.; Houston, P. L. *J. Chem. Phys.* **1987**, *87*, 1445.
(25) Heck, A. J. R.; Chandler, D. W. *Annu. Rev. Phys. Chem.* **1995**, *46*, 335.
(26) Mastenbroek, J. W. G; Taatjes, C. A.; Nauta, K.; Janssen, M. H. M.; Stolte, S. *J. Phys. Chem.* **1995**, *99*, 4360.
(27) Kim, D. Y.; Brandstater, N.; Pipes, L.; Garner, T.; Baugh, D. *J. Phys. Chem.* **1995**, *99*, 4364.
(28) Harren, F.; Parker, D. H.; Stolte, S. *Comments At. Mol. Phys.* **1991**, *26*, 109.
(29) Montgomery Smith, L.; Keefer, D. R.; Sudharsanan, S. I. *J. Quant. Spectrosc. Radiat. Transfer* **1988**, *39*, 367.
(30) Chandler, D. W.; Janssen, M. H. M.; Stolte, S.; Strickland, R. N.; Thoman, J. W., Jr.; Parker, D. H. *J. Phys. Chem.* **1990**, *94*, 4839.
(31) Janssen, M. H. M.; Parker, D. H.; Sitz, G. O.; Stolte, S.; Chandler, D. W. *J. Phys. Chem.* **1991**, *95*, 8007.
(32) Guo, H. *J. Chem. Phys.* **1992**, *96*, 6629.
(33) Dell Hammerich, A.; Manthe, U.; Kosloff, R.; Meyer, H.-D.; Cederbaum, L. S. *J. Chem. Phys.* **1994**, *101*, 5623.
(34) Amatatsu, Y.; Yabushita, S.; Morokuma, K. *J. Chem. Phys.* **1996**, *104*, 9783.
(35) Yabushita, S.; Morokuma, K. *Chem. Phys. Lett.* **1988**, *153*, 517. Amatatsu, Y.; Morokuma, K.; Yabushita, S. *J. Chem. Phys.* **1991**, *94*, 4858.
(36) Bulthuis, J.; Milan, J. B.; Janssen, M. H. M.; Stolte, S. *J. Chem. Phys.* **1991**, *94*, 7181.
(37) Bulthuis, J.; Stolte, S. *J. Phys. Chem.* **1991**, *95*, 8180.
(38) Fuglesang, C. D.; Baugh, D. A.; Pipes, C. L. *J. Chem. Phys.* **1996**, *105*, 9796.
(39) Ogorzalek Loo, R.; Hall, G. E.; Haerri, H.-P.; Houston, P. L. *J. Phys. Chem.* **1988**, *92*, 5.
(40) Penn, S. M.; Hayden, C. C.; Carlson Muyskens, K. J.; Crim, F. F. *J. Chem. Phys.* **1988**, *89*, 2909.
(41) Minton, K. T.; Felder, P.; Brudzynski, R. J.; Lee, Y. T. *J. Chem. Phys.* **1984**, *81*, 1759.
(42) Syage, J. A. *J. Chem. Phys.* **1996**, *105*, 1007.